SPECTRAL ELEMENT APPROACH TO WAVE PROPAGATION IN UNCERTAIN BEAM STRUCTURES

V. AJITH AND S. GOPALAKRISHNAN

Abstract. This paper presents a study on the uncertainty in material parameters on the wave propagation responses in metallic beam structures. Special efforts are made to quantify the effect of uncertainty in the wave propagation responses at high frequencies. Both modulus of elasticity and density are considered uncertain and the analysis is performed using Monte-Carlo simulation (MCS) under the environment of Spectral finite element method (SEM). The randomness in the material properties are characterized by three different distributions namely normal, Weibul and extreme value distribution and their effect on wave propagation, in beam is investigated. The numerical study shows that the CPU time taken for MCS under SEM is about 48 times less than that of MCS under 1-D conventional finite element environment for 50 kHz loading. The numerical results presented investigates effects of material uncertainties on high frequency modes. Even a study is performed on the usage of different beam theories and their uncertain responses due to dynamic impulse load. These studies show even for a small coefficient of variation (COV), significant changes in the above parameters are noticed. A number of interesting results are presented, which brings out the true effects of uncertainty response due to dynamic impulse load.

1. Introduction

In the last few years, we have witnessed a large improvement in the area of new material research. As a result there is a rapid growth in the use of lighter materials in aerospace and other major industries. These materials show significant variation in material properties and as a result, created a variety of structural problems in which the uncertainties in these properties play a major part in their design. Uncertainties may exist in the characteristics of the structure itself and in the environment to which the structure is exposed [Vinckenroy 1995]. The lack of good knowledge of material properties and its behavior can be categorized as the first type of uncertainty. The other type of uncertainty is due to the change in the load and support condition with the change in environmental variables such as temperature and pressure. Another important aspect, while considering the source of uncertainties, is the modeling technique. In this context, when the variability is large, we can find in the literatures available that the probabilistic models are advantageous than the deterministic ones. In probabilistic methods, uncertainty in the parameters is considered and is represented by a random variable or random field. The development in the field of digital computers has revolutionized the status of research in this area [Li and Chen 2006]. In many cases of structural design, with the availability of computational tool

Key words and phrases. MCS, SEM, Normal distribution, Weibul distribution, Extreme value distribution, Wavenumber, Group speeds.

such as Monte-Carlo simulation, uncertain analysis is incorporated in the design phase of the structures.

One of the major classification in the field of probabilistic methods in mechanics includes statistical approach and non statistical approach [Liu et al. 1986a]. Direct MCS, which involves sampling and estimation, is an example for a frequently used statistical approach and the theory of MCS is explained in references James [1980], Decker [1991] and Schueller [2001]. Techniques like random perturbation method, orthogonal polynomials expansion methods and numerical integration comes under the category of non-statistical schemes [Li and Chen 2006]. Non-statistical methods do not need the prior knowledge about the multivariate distribution of the stochastic parameters. Because of its simplicity and low computational effort, perturbation techniques are used along with the stochastic finite element method (PSFEM) in many problems in static and dynamic elastic analysis, composite ply failure problems, inelastic deformation studies, analysis of free vibration of composite cantilevers and non linear dynamics [Klieber and Hein 1992]. The simplicity and low computational cost makes PSFEM advantageous. However, in this approach, because of the use of Taylor series expansion for the approximation of the structural response, accurate results are expected only for the case of low variability of the parameters and for nearly linear problems. The method of orthogonal expansion is also used widely for a variety of structural problems [Ghanem and Spanos 2003]. In this method, the accuracy is highly influenced by the variability of parameters and the linearity of the problem. From the literature available [Li and Chen 2006, Liu et al. 1986a and Liu et al. 1986b], we can realize the inability of the non-statistical approaches to handle large variances of the random variables when compared with their mean values. Usually, the maximum bound set for the coefficient of variation is 10%. However, few researchers Liu et al. [1986b] and Ang and Tang [1975] have shown that the coefficient variation could be as high as 20% for acceptable results to be obtained . Monte Carlo method is a versatile approach, which can be applied easily to any complex problem whose deterministic solution is known [Shinozuka 1972, Spanos and Zeldin 1998 and Lepage 2006]. This method is commonly used for the prediction of eigen values of the structures [Lepage 2006]. Monte Carlo method can be coupled with finite element method with only slight modification in the parent code. Here the results converge to the correct solution as the number of simulation becomes large and hence the method is computationally expensive. Monte-Carlo solutions are usually used as reference solutions on account of the absence of inherent assumptions [Antonella and Karam 2009]. In some literature the Monte-Carlo method is used along with other methods to reduce the computational time. Among them, a compatible blend of the Neumann expansion with MCS has been found to work efficiently for computation of stochastic structural response[Basudeb and Subrata 2002]. There are also many methods of sampling available in the literature to improve the accuracy and the efficiency of the Monte-Carlo methods [Lepage 2006 and Stefanou 2002].

In the area of structural health monitoring, the wave propagation responses, which are very sensitive to small stiffness changes, is used effectively to detect small defects such as delamination, crack etc. in structures [Gopalakrishnan et al. 2008, Nag et al. 2003 and Ostachowicz 2005]. However, structures made from common structural materials exhibit

large variation in the material properties and the response to dynamic loading show significant changes in responses compared to the deterministic value. The presence of damage causes stiffness reduction, which causes the shift in the natural frequencies, especially at high frequencies [Tracy and Padoen 1989]. Variation in the material properties also shifts the natural frequencies and the modal amplitudes. Without a proper uncertain dynamic analysis, these shifts in natural frequencies can be misunderstood as one that is caused by the presence of structural damage. The deterministic wave propagation analysis in such cases will give results, which may be misleading. Hence, a detailed study on the effect of variation in the different structural parameters on the structural response, for a high frequency impact load is required to bring greater clarity to the interpretation of the obtained results. However, to the author's best knowledge not much work has been done in the area of uncertainties in wave propagation in structures. Also the high frequency response analysis, using conventional finite element method is computationally expensive since the maximum possible size of the finite element depends on the wavelength of the propagating wave [Gopalakrishnan et al. 2008 and Horr and Safi 2003]. Consequently, some of the current literature on the high frequency analysis of structural response use spectral finite element method (SEM) [Gopalakrishnan et al. 2008], which combines the accuracy of the conventional spectral methods and geometric flexibility of the finite element methods. Unlike the spectral methods in stochastic finite element method, the solution from SEM, is exact in most of the deterministic case [Gopalakrishnan et al. 2008 and Doyle 1997]. Also SEM, due to its ability to model the inertial distribution of the structure accurately, requires very small system size to model and obtain deterministic responses, especially for high frequency content loads. The speed of the wave analysis using SEM depends on the total time window required to avoid the problem due to enforced periodicity and the time window can be adjusted by changing the time sampling rate or the number of FFT points. The increase in the group speed with frequency reduces the total time window needed for the analysis, which further reduces the computational time. However, in the conventional FEM, the requirement of size of the element to be comparable with the wavelength makes the problem size so large that it becomes computationally prohibitive, especially in the context of uncertain analysis. The requirement of large computational time is the major restricting factor for the researchers to perform high frequency wave propagation analysis in the uncertain environment. In this context the reduction in computational time of SEM and the large increase in its computational efficiency over conventional FEM with the increase in frequency is a very relevant fact and is still an unexplored area of research. Incorporating Monte-Carlo simulation under SEM is straightforward. Due to its very small size incorporation of MCS under SEM, unlike conventional FEM, can no longer be considered as luxury from the computational view point. MCS under SEM can be the part of the design exercise. The versatility of the Monte-Carlo approach and the time aspect of the SEM are the major factors, which paved the way for the union of these two approaches. This will really encourage the researchers, especially in the field of uncertain wave propagation analysis and help them to save an immense amount of computational time.

The paper is organized as follows. In the next section, brief description of conventional SEM is given, which is followed by the brief description of MCS and the implementation of

SEM under MCS. This is followed by a detailed section on numerical examples. Here, first we conduct a study on the effects of uncertainties on the time domain responses. Then the computational superiority of SEM under MCS as apposed to conventional FEM under MCS, is established. Then the uncertainty analysis is performed for the frequency response functions. A section for analyzing the variation of time of arrival of first reflection with uncertainty is performed, which is followed by a study of the effect of loading frequency (for a tone burst signal) on the uncertain responses and then a detailed study on the spectrum relations. It is well known that the inclusion of higher order effects dramatically changes the deterministic response in an elementary beam and rod. Hence, a small subsection is included on the effects of different beam and rod theories on the uncertain responses. In all cases, both Young's modulus and density of structure are considered as uncertain, wherein their statistical distribution are assumed as normal, Weibul and extreme value distribution. In addition, in most cases both axial and bending responses are considered to study the effects of uncertainties, where the load histories considered are both broad band triangular loading and narrow band, modulated tone burst loading. The paper presents some interesting results on the input and output distribution of these parameters. The paper ends with a summary and conclusion.

2. Spectral finite element method

In the spectral element approach, the actual response is synthesized by a prudent combination of many infinitely long wave trains of different periods (or frequencies). Thus the governing equations are first converted to the frequency domain,using discrete Fourier transform and solved. The last step of the analysis involves performing inverse Fourier transform for reconstructing the signal to obtain the time domain responses. In SEM, the stiffness matrix is established in the frequency domain, which is its main difference from the conventional FEM. Also in contrast to the conventional FEM, the spectral elements can span all the way from one joint. Hence, SEM yields system size, which is many order smaller than the conventional FEM. More details of this approach is given in Gopalakrishnan et al. [2008]. In this section, we briefly discuss the formulation of spectral rod and beam element formulation. In the case of beams, we provide the formulation of both Euler-Bernoulli and Timoshenko beam although only Timoshenko beam model is used in all simulation.

For a rod [Gopalakrishnan et al. 2008], the governing partial differential equation is

$$EA\frac{\partial^2 u}{\partial x^2} - \rho A\frac{\partial^2 u}{\partial t^2} = 0 \tag{2-1}$$

where *u(x, t)* is the axial displacement, ρ is the density, E is the Young's modulus, and A is the area of cross section. In SEM the common procedure is to convert this governing partial differential equation in to the frequency domain and to solve the ordinary differential equations, so obtained. This is a discrete fourier transform (DFT) based analysis of wave propagation, where the DFT is performed by a FFT algorithm, popularly known as Cooley Tukey algorithm [Gopalakrishnan et al. 2008 and Doyle 1997]. The discrete Fourier transform of u is given a solution in the exponential form given by,

$$u(x,t) = \sum_{n=1}^{N} \hat{u}_n(x,\omega_n) e^{i\omega_n t}, \tag{2-2}$$

where, $\hat{u}_n(x,\omega_n)$ is the transform of $u(x,t)$, N is the number of FFT points, ω_n is the frequency at nth sampling point.

Substitution of Equation (2-2) in Equation (2-1) converts the governing PDE to ODE, which is given by,

$$\frac{\partial^2 \hat{u}_n}{\partial x^2} + k_n^2 \hat{u}_n = 0, \tag{2-3}$$

where, k_n is the wavenumber, which is given by,

$$k_n = \omega_n \sqrt{\frac{\rho A}{EA}} \tag{2-4}$$

The nature of wavenumber depends on the frequency tells about the type of wave generated by the medium. In the present case, wavenumber varies linearly with the frequency and hence the waves are non-dispersive, that is, they retain their shape as they propagate. The group speeds of propagation is obtained from the expression,

$$C_g = \frac{d\omega}{dk} = \sqrt{\frac{E}{\rho}} \tag{2-5}$$

The solution of Equation (2-3) is given by

$$u(x,t) = \sum_{n=1}^{N} [A e^{-ik_n x} + B e^{+ik_n (L-x)}] e^{i\omega_n t} \tag{2-6}$$

SEM uses Equation (2-6) as interpolating function for finite element formulation. The procedure for element formulation, assembly and solution are similar to those of finite elements and hence not reported here.

In case of beams we derive the spectral solution for Euler-Bernoulli beam. The governing equation is given by,

$$EI \frac{\partial^4 w}{\partial x^4} = \rho A \frac{\partial^2 w}{\partial t^2} \tag{2-7}$$

where, $w(x,\ t)$ is the transverse displacement, EI is the flexural rigidity, ρ is the density and A is the area of cross section. Transforming Equation (2-7) in to frequency domain using DFT, we get

$$w(x,t) = \sum_{n=1}^{N} \hat{w}_n(x,\omega_n) e^{i\omega_n t}, \tag{2-8}$$

$$\frac{d^4 \hat{w}_n}{dx^4} + k_n^4 = 0, k_n^2 = \sqrt{\frac{\omega_n^2 \rho A}{EI}} \tag{2-9}$$

$\hat{w}(x,\omega_n)$ is the transform of *w(x,t)*. We see that wavenumber is a non-linear function of frequency and hence the waves are highly dispersive. Hence the group speeds (C_g), unlike the rods, is a function of frequency, which is a characteristic of the most dispersive wave.

$$C_g = \frac{d\omega}{dk} = 2\sqrt{\omega_n}(\frac{EI}{\rho A})^{1/4} \tag{2-10}$$

Similarly, in Timoshenko beam theory the value of wavenumber can be calculated from the transformed homogeneous differential equation in the frequency domain [Gopalakrishnan et al. 2008].

$$GAK(\frac{d^2\hat{w}}{dx^2} - \frac{d\hat{\phi}}{dx}) + \rho A\omega_n^2\hat{w} = 0 \tag{2-11}$$

$$EI\frac{d^2\hat{\phi}}{dx^2} + GAK(\frac{d^2\hat{w}}{dx^2} - \hat{\phi}) + \rho I\omega_n^2\hat{\phi} = 0 \tag{2-12}$$

and the boundary conditions

$$(\hat{w}) or (\hat{V} = GAK(\frac{\partial\hat{w}}{\partial x} - \hat{\phi})), \tag{2-13}$$

$$(\hat{\phi}) or (\hat{M} = EI\frac{\partial\hat{\phi}}{\partial x}) \tag{2-14}$$

where, $\hat{w}(x,\omega_n)$ is the transform of transverse displacement, $\hat{\phi}(x,\omega_n)$ is the transform of slope, G is the modulus of rigidity, A is the area of cross section, $I$is the moment of inertia, ω_n is the frequency at nth sampling point, ρ is the density, E is the Young's modulus, $\hat{V}(x,\omega_n)$ is the transform of shear force, $\hat{M}(x,\omega_n)$ is the transform of bending moment and K is the shear correction factor (K is assumed the value 0.86 as in Gopalakrishnan et al. [2008]. Thus from the homogeneous differential equations and the boundary condition we will arrive at the characteristic equation for wavenumber computation is,

$$[GAKEI]k^4 - [GAK\rho I\omega_n^2 + EI\rho A\omega_n^2]k^2 + [\rho I\omega_n^2 - GAK]\rho A\omega_n^2 = 0 \tag{2-15}$$

Since the equation is of fourth order, we have four solutions for the wavenumber. The second wavenumber, which are associated with shear deformation, is evanescent to start with and becomes propagating at some high frequencies. The frequency at which this happens is called the cut-off frequency, which is obtained by setting the last term in the Equation (2-15) to zero, which is given by,

$$\omega_c = \sqrt{\frac{GAK}{\rho I}} \tag{2-16}$$

Elementary beam equations can be obtained by setting GAK to infinity and ρI to zero. Then the complete solution can be written in the form.

$$v(x,t) = \Sigma[R_1e^{-ik_1x} + R_2e^{-ik_2x} - R_1e^{-ik_1(L-x)} - R_2e^{-ik_2(L-x)}]e^{i\omega_n t} \tag{2-17}$$

$$\phi(x,t) = \Sigma[Ae^{-ik_1x} + Be^{-ik_2x} + Ce^{-ik_1(L-x)} + De^{-ik_2(L-x)}]e^{i\omega_n t} \tag{2-18}$$

A,B,C and D are coefficients determined from the boundary conditions and Ri are the amplitude ratios given by [Gopalakrishnan et al. 2008],

$$Ri = \frac{ik_i GAK}{GAKk_i^2 - \rho A\omega_n^2} \tag{2-19}$$

It is to be noted that Euler-Bernoulli beam predicts un realistic speeds at higher frequencies. When the beams are thick, effects of shear is significant and it converts the evanescent mode of Euler-Bernoulli beam to a shear propagating at high frequency. If this mode is not represented, properly, then it will lead to erroneous description of the dynamics of the beam. Hence all simulation in the paper are carried out using Timoshenko beam model.

In the case of higher order rod model in addition to axial deformation, we add the lateral motion through a term associated with Poisson's contraction. This theory, which is called Mindlin-Hermann theory, was first formulated for circular cross section by Mindlin and Herrmann [Mindlin and Herrmann 1950] and later extended for rectangular cross section by Martin et al, for metallic structures. The details of the element formulation, wavenumber and the group speed computation are given in Martin et al. [1994]. Here, for the sake of completeness, we provide the characteristic equation for computation of the wavenumber, which is given by

$$\begin{gathered}[2G(1+\bar{\nu})K_1GI]k^4 - [(2GA)^2(1+2\bar{\nu}) - 2GA(1+\bar{\nu})K_2\rho I\omega_n^2 - \\ K_1GI\rho A\omega_n^2]k^2 + [\rho IK_2\rho I\omega_n^4 - 2GA(1+\bar{\nu})K_2\rho I\omega_n^2] = 0\end{gathered} \tag{2-20}$$

where, $\bar{\nu}$ is the effective Poisson's ratio

$$\bar{\nu} = \frac{\nu}{(1-\nu)} \tag{2-21}$$

for plane stress problems and

$$\bar{\nu} = \frac{\nu}{(1-\nu^2)} \tag{2-22}$$

for plane strain problems,where ν is the Poisson's ratio. K_1 and K_2 are correction factors intended to compensate for the approximate form of the displacement field. Here, in this study K_1 and K_2 have been assumed the values 1.2 and 1.75 as in Martin et al. [1994].

Unlike the elementary rod, the wavenumber is highly dispersive, especially at high frequencies. The lateral contraction mode becomes propagating only at high frequencies. The cut-off frequency occurs at

$$\omega_c = \sqrt{\frac{2GA(1+\bar{\nu})}{\rho IK_2}} \tag{2-23}$$

3. Monte-Carlo simulation under Spectral finite element method

MCS is capable of giving accurate solutions for any problems whose deterministic solution is known,since it statistically converges to the correct solution provided that a large number of simulations are employed. In direct MCS, the procedure starts with the generation of sampling of the input parameters according to their probability distributions and correlations. For each input sample, a deterministic spectral finite element analysis

is performed, giving an output sample. Finally, a response sampling is obtained, from which the mean and the standard deviation of the response can be obtained.

The estimator of the response $\bar{y}$ is defined in the reference Lepage [2006].

$$\bar{y} = \frac{1}{n}\sum_{i=1}^{n} y_i, \tag{3-1}$$

where n is the number of samples and y_i is the response corresponding to the i_{th} input sample.

$$E[\bar{y}] = \mu_y, \tag{3-2}$$

and

$$Var(\bar{y}) = E[(\bar{y} - E[\bar{y}])^2] = \frac{\sigma_y^2}{n} \tag{3-3}$$

where $E[\bar{y}]$ and $Var(\bar{y})$ are the expected value (first moment) and variance (second moment) of the random variable and μ_y=$E[y]$ and σ_y^2= $E[(y-\mu_y)^2]$ denotes the unknown mean and variance of the response. Mean of the distribution gives an idea about the value about which the distribution is spread and the variance is a measure of the spread of the distribution. In most of the uncertain analysis the scatter of the distribution is measured in terms of a parameter, coefficient of variation (COV), which is the ratio of the square root of the variance of the samples to the mean of the samples. Square root of the variance is also called standard deviation. The parameter, which we use in this study, as a measure of the scatter of the distribution, is COV. COV of an output parameter can also be used to measure the sensitivity of the input parameter by computing the ratio of COV of output to COV of input. Many such studies are carried out in this paper by considering wave parameters such as wavenumber, speeds, cut-off frequency etc. as output parameters and then sensitivity to the material properties are investigated.

In wave propagation analysis, this y can be the transform of time response of axial and transverse velocity, frequency response functions, wavenuber, group speed etc.. Each value of y_i is obtained using the deterministic spectral finite element code or by conventional finite element code (for the comparative study) each time.

4. Numerical Results and discussions

There are many factors that govern the wave propagation response in a structure. Some of the key factors are (a) the wavenumber (b) the group speeds (c) natural frequency of vibration and the phase information. All the factors depend on the material property of the medium in which these waves propagate. Since the material properties in this study are considered uncertain, one can expect substantial changes in the wave responses as compared to the deterministic responses. Hence, the aim of this section is to bring in the effects of uncertainty in the material properties on wavenumbers, group speeds, and the natural frequency of the system. The uncertain responses are shown in the form of time histories of velocities, frequency response function (FRF) or the probability density distribution, in order to bring out clearly the effect of uncertainty in these parameters. Both broad band and modulated high frequency tone-burst loading is considered in this study. In particular, the effect of loading frequency on the uncertain response is investigated.

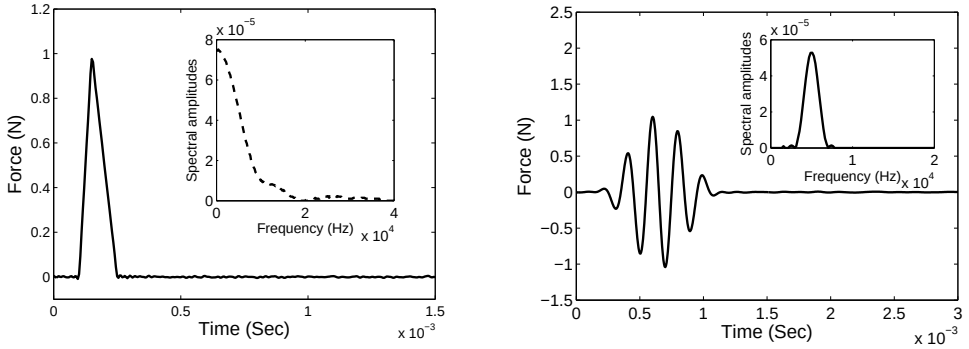

FIGURE 1. Input force used in simulation. (a) Broad band pulse (b) Narrow band modulated (at 5 kHz) pulse .

The last but not the least, the effect of using higher order theories on the uncertain response is investigated. It is quite well known [Gopalakrishnan et al. 2008] that higher order effects in rods and beams manifest itself in such a manner that it introduces cut-off frequency in the higher order wave modes, which becomes propagating beyond the cut-off frequency. The cut-off frequency depends on the material properties and geometric properties and it occurs at high frequencies. If this cut-off frequency occurs at a frequency, which is beyond the point of interest one can still use elementary beam model for the analysis. The uncertainty in material properties or geometric properties or both of them, can affect its value. Hence, a detail uncertain analysis is required, which is undertaken in this section. Here, each result is obtained by the method of MCS coupled with SEM, as discussed in the previous section. In this work the uncertainty is modeled by representing the uncertain parameters by a random variable and with different probability distribution functions to compare the pattern of distribution of the output parameters. Here, the input random variables are created using MATLAB expressions for creating a random variable. The spectral elements used for the metallic beams and rods are similar to the type, which we find in the reference Gopalakrishnan et al. [2008].

First a comparative study of the effect of axial and transverse response of the metallic beam is performed, between the conventional FEM and the SEM, for a normal distribution and for different coefficient of variation of the Young's modulus and the density. Then, variation in the frequency responses, speed and the wavenumber are also analyzed to investigate about the variation of these output parameters as discussed previously.

4A. **Effect of uncertainty on Velocity Time histories.** In this study, we consider a cantilever metallic beam of 1 m. length with a rectangular cross section 10 mm x 10 mm. The beam is modeled using single Timoshenko beam and elementary rod (in the SEM case) and 200 1-D beam and rod elements are used in the case of conventional FEM. The deterministic value of Young's modulus and density are 70 Gpa and 2700 kg/m^3 respectively. The objective here is twin fold, first we will compare the axial and

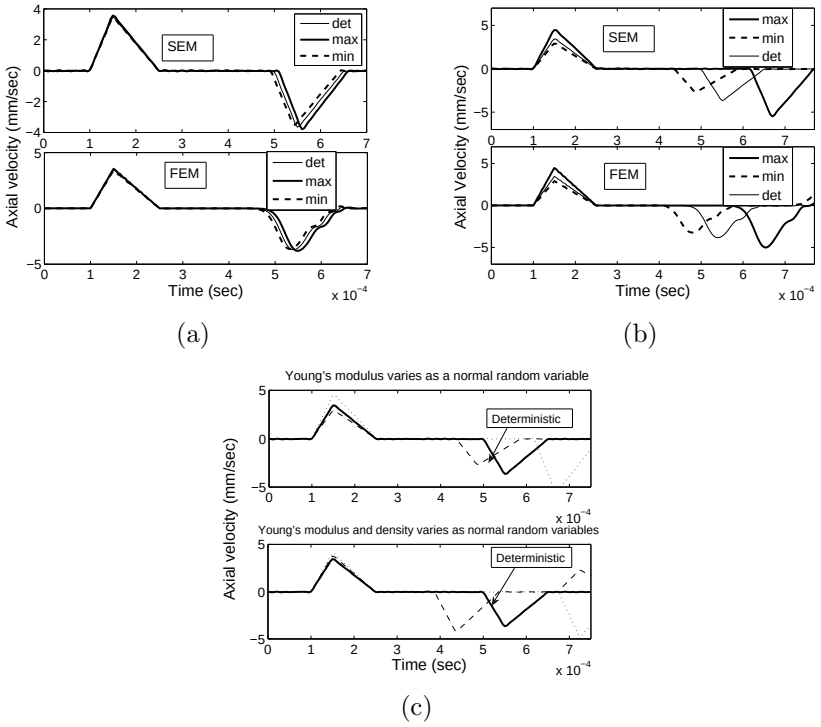

FIGURE 2. Axial velocity responses. (a) Uncertain Young's modulus with COV 1% (b)Uncertain Young's modulus with COV 10% (c)Uncertain Young's modulus and Density with COV 10%.

flexural response predicted by conventional FEM and SEM to validate the latter and, the second is to quantify the response changes due to material uncertainties. For FEM and SEM comparison, we assume only Young's modulus as uncertain with an assumed normal distribution. Ten thousand randomly generated samples of Young's modulus is used in the simulation. In most of the uncertain analysis, the mean of a parameter obtained from the simulated data should converge to a constant value. This requires large number of samples and from our study we found that 10000 samples are required to satisfy this condition. For comparison of SEM and FEM solution, two different input, as shown in Figure 1 is used. Figure 1(a) is a broad band loading, whose FFT gives a frequency content of 20kHz. This pulse is used in the case of axial wave propagation. Flexural waves are highly dispersive in nature. This is due to the dependence of group speeds of the waves on the frequency. One of the ways to make signal travel non-dispersively in a beam is to use a tone-burst modulated pulse, shown in Figure 1(b), modulated at 5 kHz frequency. The FFT of the pulse also shown in the inset of the figure has significant energy only at 5 kHz and hence, the waves travel at a speed corresponding to 5 kHz. We use this pulse for flexural wave propagation. First we consider Young's modulus as random variable and MCS is performed both under conventional FEM and SEM environment using 10000 samples. Here, in each figure the legend "min" and "max" signify the minimum and maximum

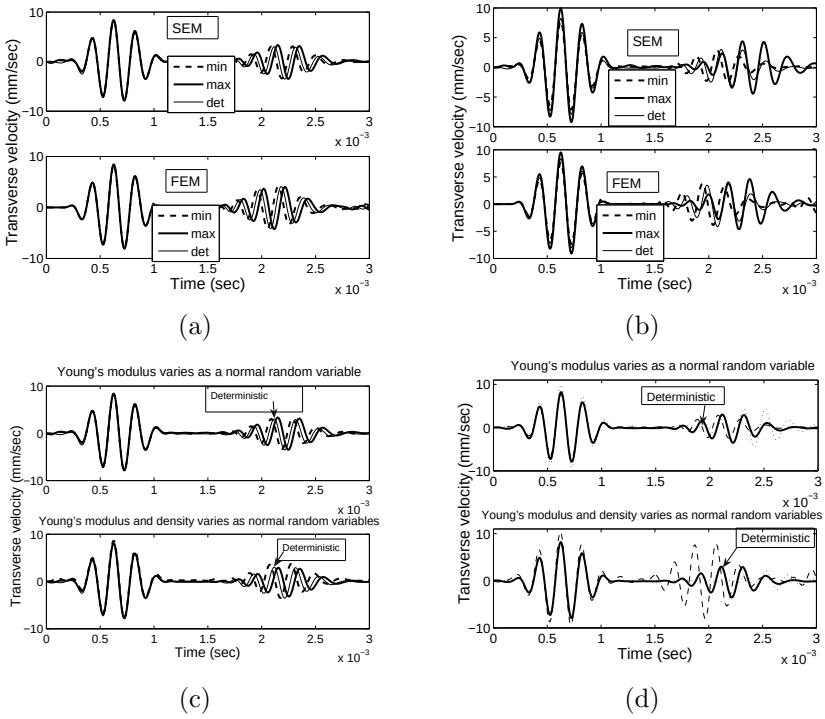

FIGURE 3. Transverse velocity responses. (a) Uncertain Young's modulus with COV 1% (b) Uncertain Young's modulus with COV 10% (c) Uncertain Young's modulus and Density with COV 1%(d) Uncertain Young's modulus and Density with COV 10%.

value of time of arrival of the first reflection obtained through MCS and "det" is its value, when the material properties are deterministic. Figure 2(a) and Figure 2(b) shows the axial velocity history obtained with input parameter COV 1% and 10% respectively. Two things are quite apparent from the figure. First the prediction made by MCS under FEM and SEM match very well. The second is that if the COV is small, the uncertain response does not deviate much as compared to the deterministic response. Since the group speed of the medium depends on the material properties, uncertainty in material properties can cause changes in the predicted group speeds, which can be quantified by looking at the time of arrival of the first reflection. From Figure 2(b), it is clear that the total scatter in the time of arrival of first reflection is 15%, compared to its value in the deterministic case, for a COV of 10 % , which in terms of speed will be around 2000 m/sec. There is a significant increase in group speed introduced by uncertainties in material properties.

Figure 3(a) and Figure 3(b) shows the flexural responses obtained through MCS under FEM and SEM as a function of COV. As in the case of axial waves, FEM and SEM predictions match well. Unlike the case of axial wave propagation, for larger COV, the scatter induced in the flexural group speeds are not that significant. Next, both Young's modulus and density are made uncertain and we assume normal distribution for both

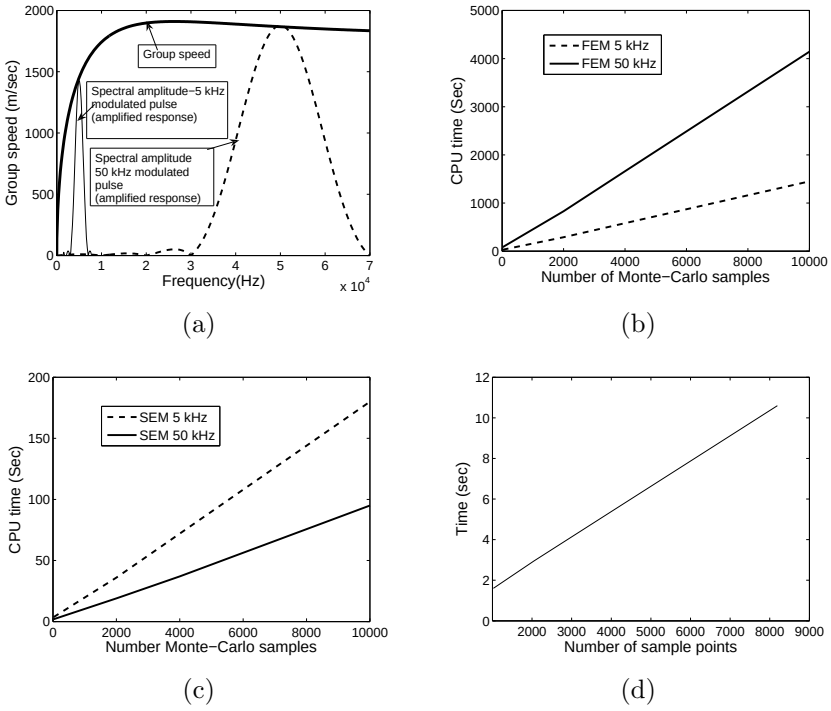

FIGURE 4. (a) Dispersion plot(bending group speed) of the beam, where the spectral amplitudes(amplitudes are amplified) of 5 kHz and 50 kHz tone-burst signals are superimposed to it, CPU time as a function of number of samples for different ton-burst signal frequencies (5 kHz and 50 kHz) with (b)FEM (c) SEM and (d) SEM for different number of FFT points for 100 samples.

these parameters. Figure 2(c) and Figure 3(d) shows respectively, the axial and transverse velocity histories for a case of 10% COV, obtained through SEM. From these figures, it is clear that significant changes in the group speeds are introduced both in the axial and flexural cases, where the total scatter in axial speed is about 25% and flexural speed is about 20% when compared to the deterministic responses. In terms of speed, this change amounts to change in group speed of 3450 m/sec (for axial) and 350 m/sec (for the flexural case). Figure 3(c) is the flexural response for a case of COV 1%, from which it can be concluded that the variation in the time responses with the change in the number of input random variables from one to two is significantly less, when the COV of input parameters are less. In summary, uncertainty in material parameter increases the total scatter in the group speeds. If modulus alone is uncertain, then the flexural group speeds does not change significantly. However, when both density and modulus are uncertain, flexural group speeds shows a total scatter of nearly 20% with 10% COV in the input parameters. The variation in the time responses with the change in the number of input random variables from one to two is significantly less when the COV of input parameters are less.

4B. **Comparison of efficiency of FEM and SEM using Monte-Carlo simulation.** Here, to determine the efficiency of SEM under MCS, the same cantilever beam of the previous example is considered. The beam is modeled as a single Timshenko beam. Two different tone-burst loading, one samples at 5 kHz and other at 50 kHz are used for the study. Figure 4(a) shows the bending wave speed super imposed with the FFT spectrum of 5 kHz and 50 kHz loading. 5 kHz load will travel at 1400 m/sec while the 50 kHz pulse will travel at 1900 m/sec according to the figure. This means 50 kHz pulse will travel faster than the 5 kHz loading. Hence, the reflection will arrive earlier in 50 kHz loading, which manifests itself to having smaller time window as compared to 5 kHz loading. In other words 50 kHz tone-burst loading needs smaller time window, which means smaller number of FFT points as compared to 5 kHz ton-burst loading. Hence, we can expect faster SEM solutions for 50 kHz loading as apposed to 5 kHz loading.

In conventional FEM, when the frequency increases, the wavelength decreases and the conventional FEM mandates that the element length should be comparable to its wavelength, as in Chakraborty and Gopalakrishnan [2004], and typically, 6-10 elements should span a wavelength. Hence, increase in loading frequency, increases the problem size in conventional FEM, which will certainly increase the analysis time. This is quite in contrast to SEM solution. In the present case, increase in the frequency from 5 kHz to 50 kHz, increases the number of conventional elements required from 200-600 elements. Figure 4(b) and Figure 4(c) shows the comparison of the time taken by the Monte-Carlo simulation under FEM and SEM as a function of number of samples, for the transverse velocity response of a cantilever beam, using two different tone burst signals. In spectral FEM, a time sampling rate of 5 μs with 1024 FFT points are used for a 5 kHz signal loading and the number of FFT samples used for a 50 kHz load is only 512. Conventional FEM uses 200 1-D beam elements, for a tone-burst pulse of modulated frequency 5 kHz and 600 elements, for a tone-burst pulse of frequency 50 kHz. Only Young's modulus is assumed as random variable and the randomness is modeled as normal distribution. From these figures, we can clearly see, SEM is faster as compared to conventional FEM, for both loadings. SEM is 8 times faster for 5 kHz loading and takes less than 200 seconds to compute the responses. The factor increases from 8 to 48, when the frequency content of the load is 50 kHz. Hence, MCS under SEM cannot be thought of as a luxury under SEM.

One of the problems associated with SEM is that it cannot handle finite small dimension structure, which is due to enforced periodicity in the frequency domain used in the DFT. The enforced periodicity causes the responses to wrap around due to its inability to damp out all the responses within the chosen time window. To overcome this, we need to enlarge the time window, which can be done either by increasing the time sampling rate or by increasing the number of FFT points or both. In the present case, for a 100 sample MCS simulation the time taken by SEM as a function of number of FFT points are shown in Figure 4(d). The CPU time variation is linear an is quite small. In summary SEM performs the simulations faster than the conventional FEM, which increases with the increase in the frequency content of the load.

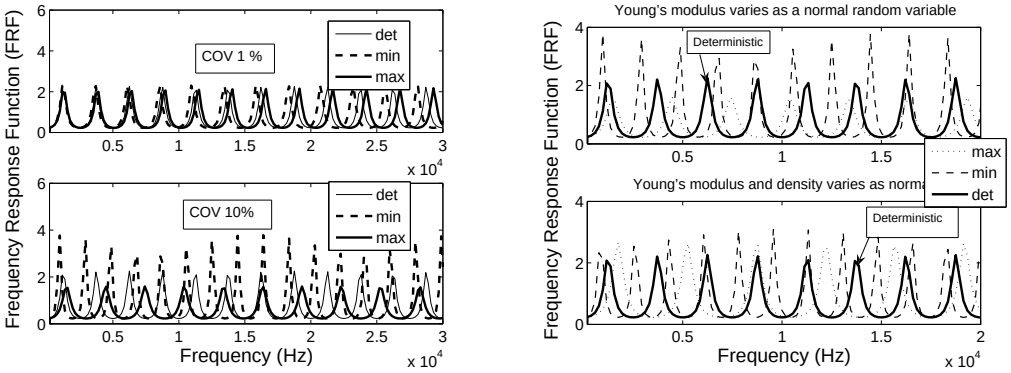

(a) (b)

FIGURE 5. FRF of Axial modes for 1% and 10% COV. (a) Young's modulus is uncertain (b) Both Young's modulus and density uncertain (COV 10%).

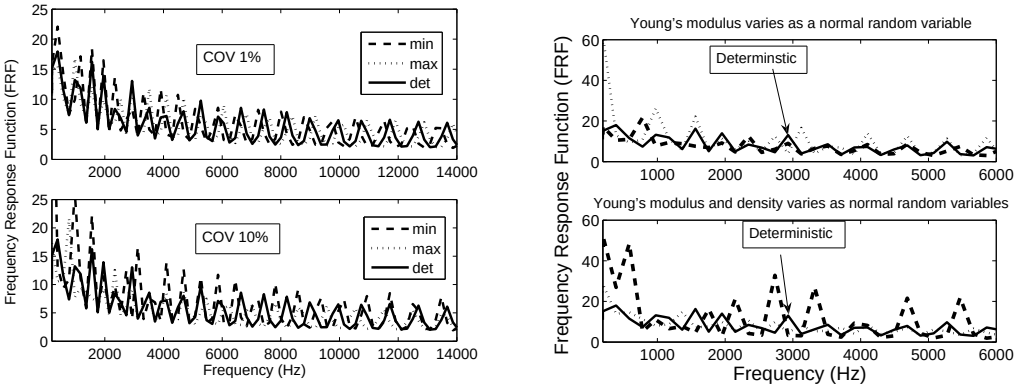

(a) (b)

FIGURE 6. FRF of flexural modes for 1% and 10% COV. (a)Young's modulus uncertain (b)Both Young's modulus and Density uncertain (COV 10%).

4C. **Effect of variation on natural frequencies and modal amplitudes.** Natural frequencies are functions of material properties. If these properties are uncertain, then we will see significant variation in the responses predicted by the analysis. In particular, shift in the natural frequency is used as a way to assess the presence of damage in the structure. There exists a difficulty in distinguishing the shift in the natural frequency due to damage with shift in frequencies due to material uncertainties, which makes it necessary to perform a detailed uncertainty analysis. SEM directly gives the FRF as a by product, a plot of which will provide us the insight on how the frequencies are shifting due to material uncertainties.

We first consider a single elementary rod spectral FEM model, fixed at one end. In the first case we consider Young's modulus alone is uncertain with its mean value at 70 Gpa and over 10000 samples are used in the MCS. Here, in this study we assume only normal distribution for all the input random variables. Figure 5(a) shows the FRF for a rod for 1% and 10% COV in the input parameter, Young's modulus. For 1% COV the shift in the first three mode are very small and thereafter, there is some increase in the shift. All modes exhibit negligible change in the modal amplitudes. This is also a typical behavior of a metallic beam with small cracks. If the COV is increased to 10%, then even the fundamental axial modes also changes and the shift in the second and higher frequencies are quite substantial. The changes in the modal amplitudes are also significant.

Next, we plot the FRF for axial loading, when both Young's modulus and density are considered random, as a function of increasing percentage of COV. This is shown in Figure 5(b). The notable feature here is that even though the shift in the natural frequency increases drastically the modal amplitudes changes not much from the deterministic values.

Figure 6(a) and Figure 6(b) shows the beam FRF, which is modeled as single Timoshenko beam for the case of Young's modulus being random and both Young's modulus and density being random, respectively. For the case of random Young's modulus, with 1% of COV, as in the case of rods, there is not much shift in the lower modes. Here, in the case of a beam model, the change in the fundamental modes and the modal amplitude with the increase in COV to 10% is observed, as in the case of a rod. Figure 6(b) shows FRF, when both Young's modulus and density are uncertain for a COV of 10%. When compared to the FRF with only Young's modulus is uncertain, significant shift are visible for the natural frequencies. However, modal amplitudes nearly double for most of the modes.

In summary, the frequency shift for a small COV for both axial and flexural mode are very small for lower order modes, while the higher modes exhibit significant shifts. Higher COV, not only show higher shift for the entire natural frequency spectrum, but also show higher modal amplitudes.

4D. **Distribution of Time of arrival of first reflection.** In section 4A, we showed that the material uncertainties significantly changed the group speeds, where in the group speed effects are quantified by computing the speeds using the time of arrival of first reflection. In this section, we would like to quantify the group speed changes in terms of distribution of time of arrival of first reflection for 2 different input material property distribution, namely, normal and extreme value distribution. The extreme value type I distribution based on the smallest extreme values is used in this study. This is also refereed to as the Gumbel distribution. In this case, only flexural response is considered, where the cantilever beam is modeled as a single Timoshenko element subjected to point impact load (Figure 1). As before 10000 samples are used in MCS. The objective here, is for an input COV of material variation, to determine the COV of time of arrival of first reflection.

Here, in each figure, the legend "Monte" means that the actual histogram from MCS and "Normal" and the "Extreme" are the ideal normal and extreme value distributions with the sample mean and standard deviations obtained from the simulated data. Figure

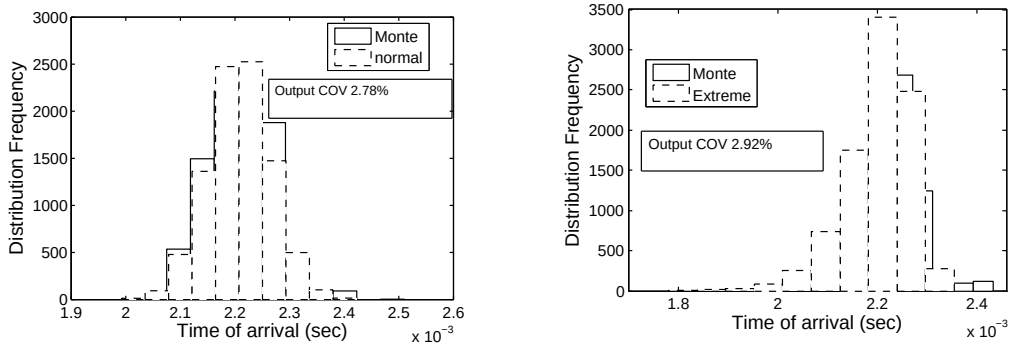

(a) (b)

FIGURE 7. Histogram of distribution of time of arrival of first reflection, Young's modulus with an input COV 10% for different distributions. (a) Normal (b) Extreme value distribution.

7 shows the distribution of time of arrival of first reflection for 2 different distribution of Young's modulus with a COV of 10%. Here, density is assumed to be deterministic. The different input distribution predict similar COV (about 2.9%) of the output. Next, we assume both density and Young's modulus as uncertain and these distributions are modeled by normal and extreme value distribution with a COV of 10%. As in the previous case, the COV remain constant (around 3.9%), for different distributions (Figure 8). For the different distribution, we see that the maximum and minimum limit of output distribution does not have significant difference. In summary, different distribution of material uncertainty does not alter the total bound of variation of group speed significantly.

4E. **Effect of loading frequency in the time responses with uncertain material properties.** A tone-burst modulated signal (Figure 1(b)) is normally used in the structural health monitoring studies to detect the presence of cracks in structure since they travel non-dispersively. These signals are modulated at certain frequencies, which depend on size of cracks, that is smaller the damage, larger will be the value of modulated frequency. The aim of this subsection is to understand and estimate the extend of shift in the arrival of first reflection that is caused by material uncertainty for increasing value of loading frequency. This aspect is very critical in health monitoring studies to distinguish clearly the shift in the arrival of first reflection caused by damage with that of the material uncertainties.

We again model the same cantilever beam of previous section with a single Timoshenko beam model and subject this beam to a tone-burst signal (Figure 1(b)), whose modulated frequencies are varied from 5 kHz to 50 kHz. In each case, results were obtained considering Young's modulus as uncertain and both Young's modulus and density as uncertain. In both these cases COV was fixed at 10%. Figure 9(a) and Figure 9(b) shows the velocity history response for 20 kHz and 50 kHz respectively. As in the earlier studies, in both the cases, the shift in the arrival of first reflection is maximum when both young's modulus

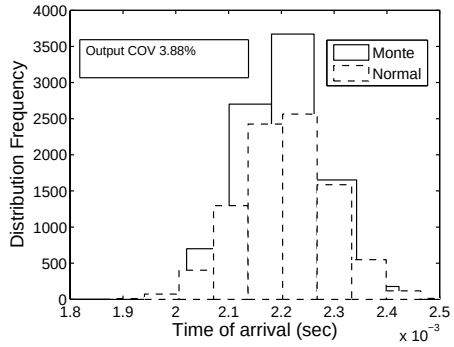

(a)

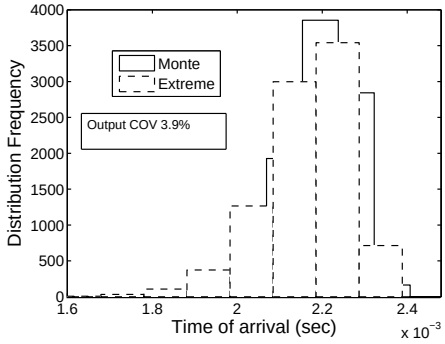

(b)

FIGURE 8. Histogram of distribution of time of arrival for first reflection with uncertain Young's modulus and Density with a cov of 10% for different distributions. (a) normal (b) extreme value distribution.

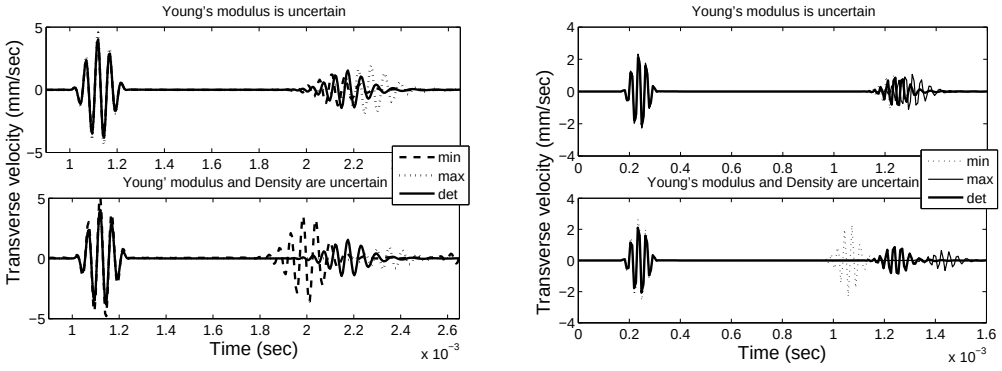

(a) (b)

FIGURE 9. Transverse velocity variation with the change in the modulation frequency. (a) 20 kHz loading (b) 50 kHz loading

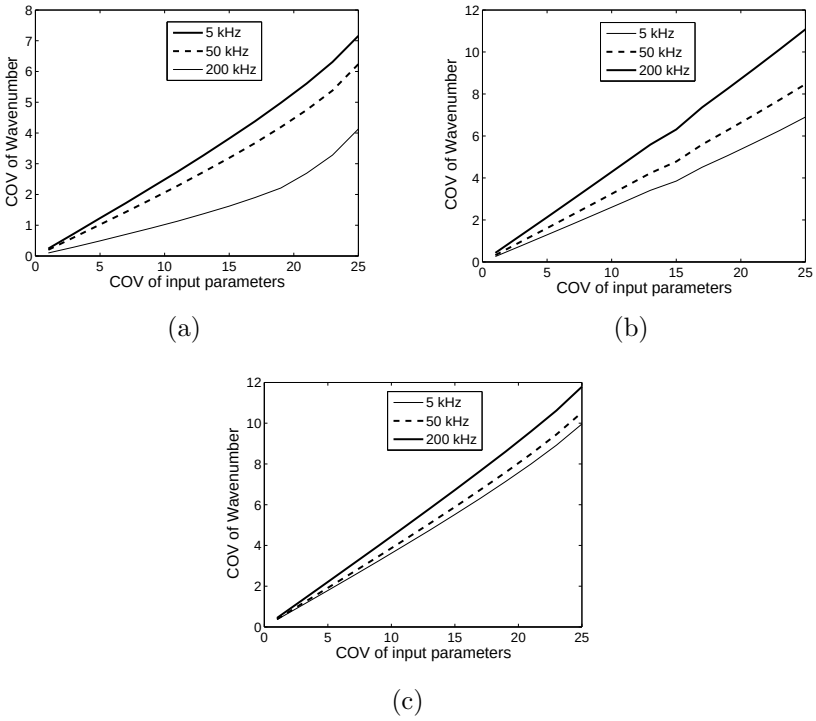

FIGURE 10. Variation of COV of wavenuber (flexural) with frequency where, input parameters varying as a normal random variable. (a)Young's modulus (b) Density (c) Young's modulus and density.

and density is uncertain. For 20 kHz loading, the variation in group speed is about 720 m/sec and this variation decreased to 660 m/sec for 50 kHz loading. When we quantify these variations in group speed, in terms of the percentage of its deterministic value, we can see an increase in the variation of group speed from 27% to 35.5% with the increase in the loading from 5 kHz to 20 kHz. However, for the loading with a frequency of 50 kHz, the variation in group speed is about 35.5%. Beyond 50 kHz, no further appreciable change in the group speed is noticed. Hence, in the health monitoring studies, it is always necessary to use signals modulated at frequencies beyond 50 kHz, if the structure is uncertain, so that the shift in reflected pulse due to material uncertainties can be factored in the damage location computation.

4F. **Wavenumber COV for different material property distribution.** Generally, in wave analysis the parameter wavenumber, which acts as a scale factor on the position variable in the same way that the frequency acts on the time (Equation 2-6, Equation 2-17 and Equation 2-18) and its variation with frequency is a major area of study. Uncertainties in material parameters scatters the waves that are quite different compared to deterministic beam. This scatter will be quite different in the presence of flaw such as cracks, especially when the parameters are uncertain. Two parameters that will help us to differentiate the scattering of waves due to material uncertainties and the damage

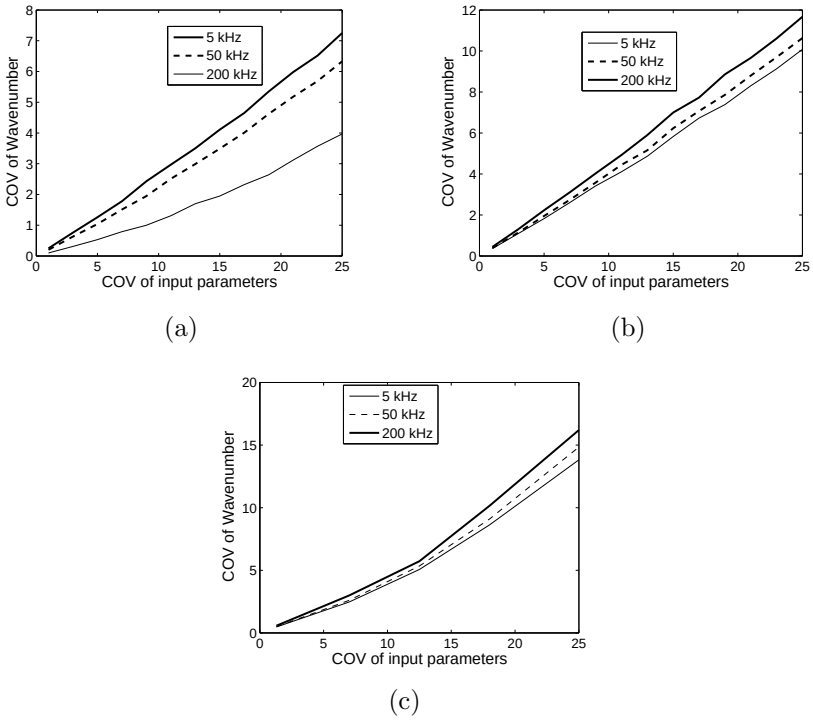

FIGURE 11. Variation of cov of wavenuber (flexural) with frequency where, input parameters as a Weibul and extreme value random variable.(a) Young's modulus (Weibul) (b) Young's modulus and density(Weibul) (c) Young's modulus and density (extreme value distribution).

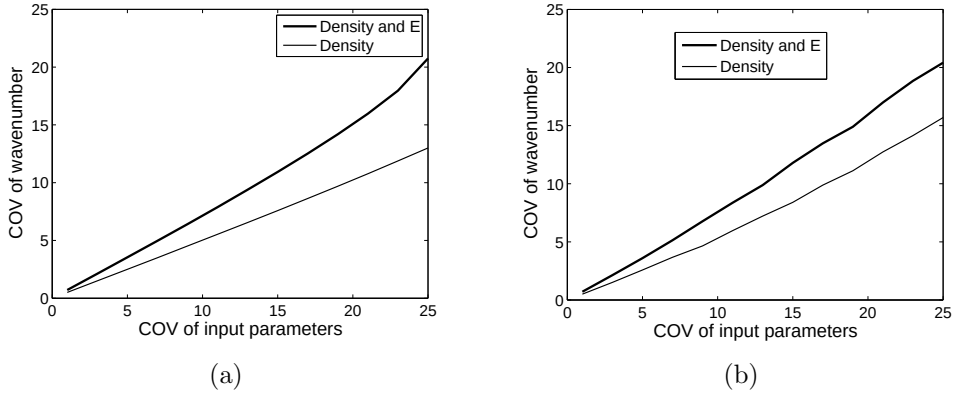

FIGURE 12. Variation of cov of wavenuber (Axial) input parameters (Density and Young's modulus) varying as(a) Normal and (b) Weibul random variable.

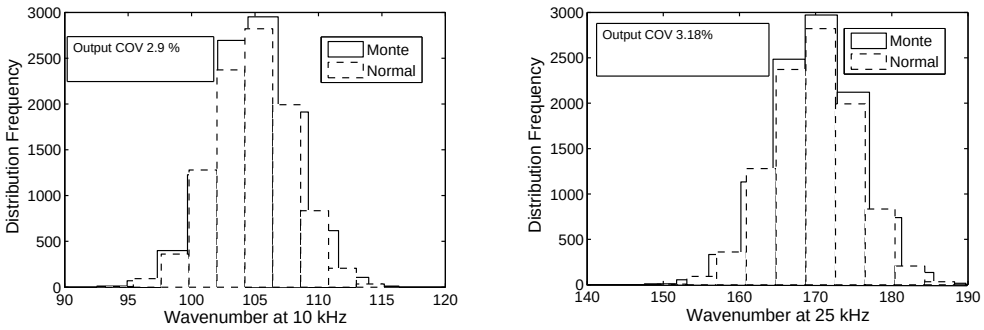

(a) (b)

FIGURE 13. Histogram of distribution of wavenumber (flexural) at different frequencies, both uncertain density and Young's modulus modeled as normal random variable with COV 7%. (a) 10 kHz (b) 25 kHz.

are the wavenumber and group speed of waves. In the application of wave propagation analysis for structural health monitoring, the time of arrival of first reflection is an important parameter, which directly depends on the group speed of the structure. However, we know that there is a direct relation between wavenumber and group speed and is given in Equation 2-5. It is very essential to study the variation of wavenumber with the variability of the material properties, which will actually help us in structural health monitoring by giving us an insight into the type of variation of group speed and its dependence on the wavenumber. In this study, we try to quantify the variation of COV of wavenumber with the variation of COV of the input parameters.

Here, we have assumed the material properties (modulus and density) to vary as normal distribution, Weibul distribution and, extreme value distribution. The wave number for beam is calculated by solving the characteristic equation, Equation (2-15), while for rod, Equation (2-4) is used. As before, 10000 randomly generated samples are used in the analysis. Figure 10 shows COV plots as a function of a few discrete frequency for normal distribution of material property. From the figure, following observation can be made. When Young's modulus alone is uncertain (Figure 10(a)) wavenumber COV variation decreases with increase in frequency on the other hand, if the density alone is uncertain (Figure 10(b)), wavenumber COV variation is just the reverse of the previous case. Figures 11(a) and 11(b) shows the flexural wavenumber COV variation for Weibul distribution. These variation pattern follow that of the normally distributed wavenumber COV. The effect of frequency on the COV of wavenumber is not noticed in a simple rod and beam model, where the term containing frequency, which is present in both denominator and numerator of the expression for COV, will cancel out each other. However, in a Timoshenko beam model the frequency has an effect in the variability of the wavenumber, which is explicit from the constant term (third term) of the characteristic equation (Equation 2-15). From the above two cases and also from the extreme value distribution of the input parameter, when both Young's modulus and density are uncertain ((Figure 10(c), Figure

11(b), Figure 11(c)), the wavenumber COV is not heavily influenced by the frequency. In fact, as compared to the case of a single uncertain input variable, in all these cases the variability in the wavenumber is very high even in the low frequency range, when the Young's modulus and density are uncertain. Figure 12 shows the wavenumber COV for axial wavenumber. The figures show, axial wavenumber COV is more than that of flexural wavenumber COV for a given material distribution and in contrast to the flexural case, wavenumber COV does not show any variation with frequency.

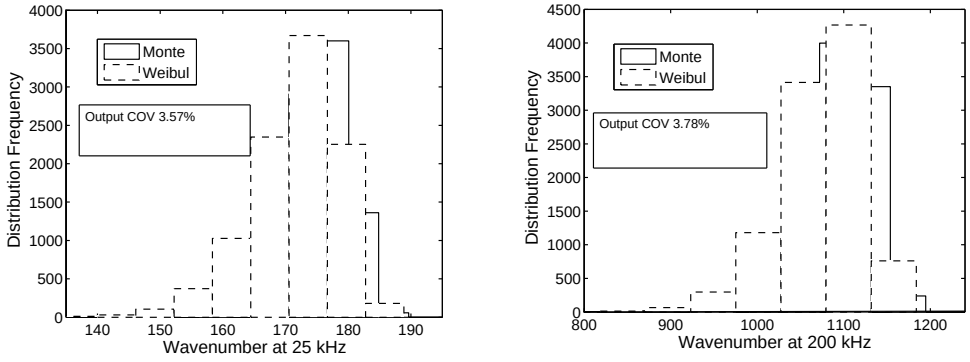

(a) (b)

FIGURE 14. Histogram of distribution of wavenumber (flexural) at different frequencies, both uncertain density and Young's modulus modeled as Weibul random variable with COV 7%. (a) 25 kHz (b) 200 kHz.

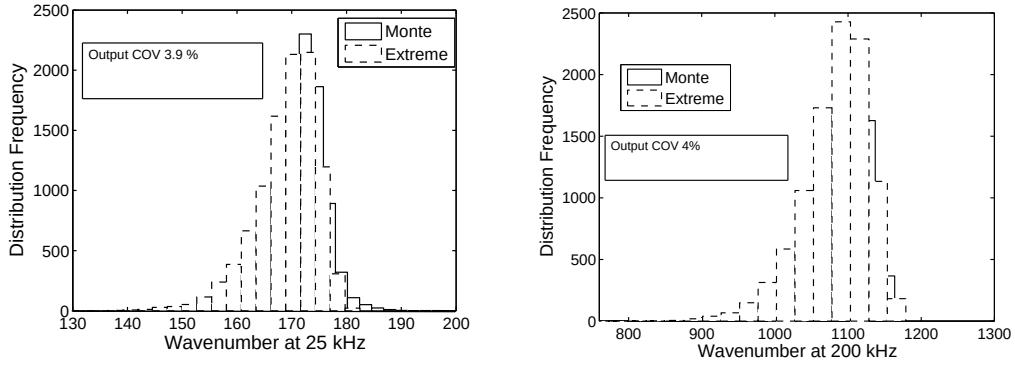

(a) (b)

FIGURE 15. Histogram of distribution of wavenumber (flexural) at different frequencies, both uncertain density and Young's modulus modeled as Extreme value random variable with COV 7%. (a) 25 kHz (b) 200 kHz.

4G. **Distribution of Wavenumber, for different types of input distributions.** In the next few plots, the variation of the wavenumber, by taking different probability density

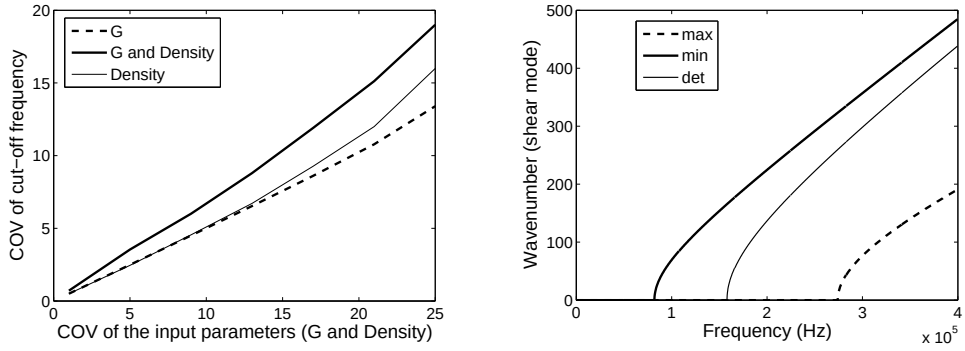

(a) (b)

FIGURE 16. Variation of cut-off frequency of the shear mode of Timoshenko beam, with uncertain rigidity modulus and density for a normal with COV 20%. (a) Variation of COV (b) Maximum and minimum bounds of cut-off frequency.

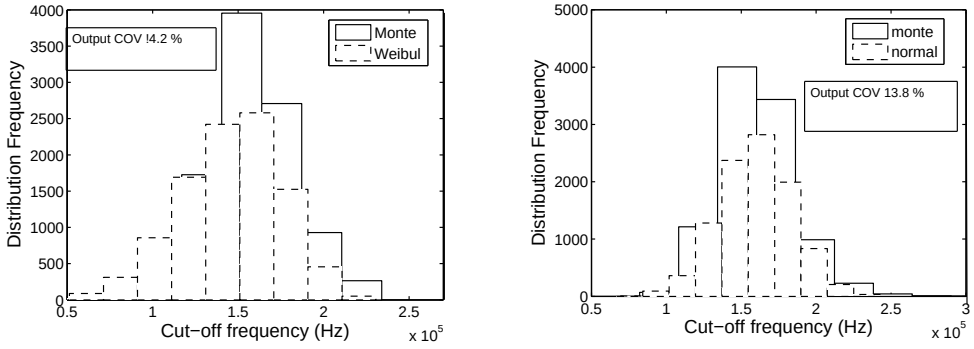

(a) (b)

FIGURE 17. Histogram of distribution of cut-off frequency of the shear mode of a Timoshenko beam, both density and rigidity modulus uncertain using different input distribution with a COV 20%. (a) Normal input distribution (b) Weibul input distribution.

function for the input parameters are shown to quantify the effect of material uncertainty. Here, we are only studying the variation in the flexural wavenumber and the uncertain input parameters considered are Young's modulus and density. Figure 13(a) and Figure 13(b) shows the change in the variation distribution of the flexural wavenumber at 10 kHz and 25 kHz, by taking the input parameters as a normal random variable with COV 7%. MCS is performed using 10000 samples and the corresponding normal distribution of the output samples are obtained using the estimates of the MCS, for the purpose of comparison. In Figure 14(a) and Figure 14(b) the input parameters are taken as Weibul distributions and in Figure 15(a) and Figure 15(b) the input parameter uncertainty is

represented as extreme value distribution. Here, the different discrete frequencies, where the wavenumber is calculated, are 25 kHz and 200 kHz. Similar to the previous case here, the corresponding Weibul and extreme value distribution of the output are obtained using the estimates of the MCS. The results shows that the distribution of variation of the wavenumber at a particular frequency, does not vary much with the change in the type of probability distribution functions and the the minimum and maximum limit obtained is almost similar in all the cases, regardless of the type of distribution considered. Moreover, it can be seen that the COV of the variation of the wavenumber is not varying much with the increase in the corresponding frequency.

4H. **Effect of uncertainty on wavenumber due to higher order effects in metallic rods and beams.** We have discussed in detail, the computation of wavenumber in section 2. In elementary rod, there is only one mode due to axial deformation, which is propagating. The wavenumber varies linearly as frequency and hence they are non-dispersive. This model was used in all the earlier simulation. Elementary beam, on the other hand has wavenumber, which are non-linear functions of frequencies and hence dispersive. It has two modes, one of which is propagating and the other is evanescent. Introducing higher order effects in to these elementary model completely alters the wave mechanics. The lateral higher order effects in rod is introduced by adding an additional lateral motion attributed due to Poisson's ratio. The wavenumber computation for the model is given in section 2. Higher order effects introduces an additional propagating mode beyond a certain frequency called cut-off frequency, which occurs at very high frequencies. In fact, existence of cut-off frequency determine the usage of a particular rod model, elementary or higher order model. That is, if the frequency of interest falls below the cut-off frequency, one can still use elementary model for analysis. Similarly, higher order effects in beam can be introduced through the introduction of shear deformation, which makes the evanescent mode propagating after certain cut-off frequency. The cut-off frequency is governed by the material properties and the geometric properties of the structure. In light of the fact that the uncertainties involved in the determination of material properties of a real structure is more, first we focused our study on the variation in the cut-off frequency of the structure with the variability in the material properties. Here, the geometric properties of the system are considered deterministic, which never initiate a higher order effect in the system. However, if the material properties are uncertain, the predicted cut-off frequencies may be quite misleading in deciding the type of analysis to be used.The aim of this section is to determine the range of shift in the cut-off frequencies due to material uncertainties so that proper theories can be used in the simulation process.

Figure 16(a)) shows the variation of the cut-off frequency with the change in COV of the input parameters (Density and G). When the number of random variables used increase from 1 (Density or G only) to two (both Density and G), we can see that the COV of cut-off frequency increases. The variation of COV of the cut-off frequency is more, when the input random variable is density, especially when the COV of input is high. Figure 16(b)) shows the upper and lower bounds of the shear mode when the COV of input random variable is 20% and the number of random variable is two (Density and G). There is a variation from the deterministic value, 161 kHz to 78 kHz, in the Lower

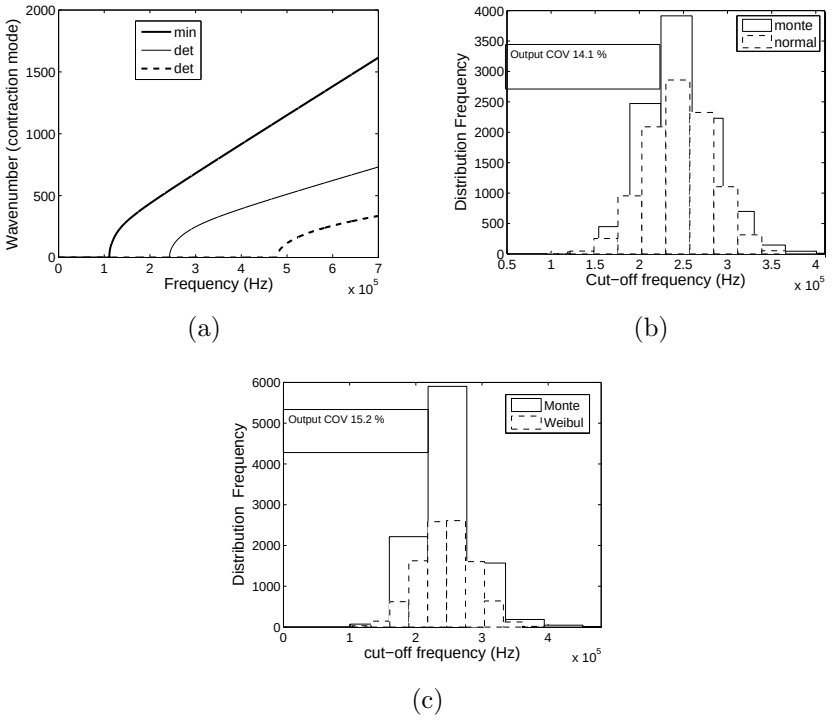

FIGURE 18. Variation of cut-off frequency for a Higher order rod for Uncertain density and rigidity modulus, with COV 20% for different distributions (a) Maximum and minimum limit for normal, Histograms of distribution of cut-off frequency for input distributions (b)normal (c)Weibul.

limit and 271 kHz, in the upper limit. The lower limit of this result suggests that, when there is such a large variation in the input parameters, there is a chance for the shear mode to propagate at lower frequency (here it is 78 kHz) than the expected frequency (161 kHz), which cannot be traced by a simple Euler-Bernoulli theory even for a thin beam. The distribution of the cut-off frequency for different distributions are shown in, Figure 17(a), Figure 17(b). We can see the output distribution variation is almost same with two distributions considered and it differs from the corresponding input distribution pattern in both the cases, where the input parameters are taken as a normal distributions and as Weibul distributions.

Figure 18(a), shows the variation in the contraction mode of a higher order rod. From the figure, we can see the deterministic value of cut-off frequency for a higher order rod is very much higher than that of the previous case of higher order beam. The uncertain response has the same impact, as in the case of the beam, in the maximum limit (here,123 kHz) of frequency of the load, which can be used with the simple elementary rod model. The distribution of the cut-off frequency is showing a same pattern of distribution as that of the beam model (Figure 18(b), Figure 18(c)). Finally the tables, Table 1 and Table2, give us an idea of the total bound of variation of the cut-off frequency of a Timoshenko

beam and a higher order rod respectively, with the change in the COV of the input parameter, when both Young's modulus and density are uncertain.

TABLE 1. Total bound of variation of cut-off frequency with different COV of input, when both Young's modulus and density are uncertain, for a Timoshenko beam (kHz)

	normal		weibul	
COV(%)	Maximum	Minimum	Maximum	Minimum
1	165.74	157.25	158.44	149.02
5	185.48	141.32	173.07	134.35
10	216.86	126.11	198.22	112.34
15	246.62	98.58	223.69	85.24
20	271.24	78.12	245.54	67.33

TABLE 2. Total bound of variation of cut-off frequency with different COV of input, when both Young's modulus and density are uncertain, for a Higher order rod (kHz)

	normal		weibul	
COV(%)	Maximum	Minimum	Maximum	Minimum
1	278.66	262.82	280.74	260.47
5	314.21	233.04	327.71	229.84
10	364.65	201.93	395.65	191.93
15	398.69	168.42	423.69	152.42
20	455.38	123.46	495.53	98.34

5. CONCLUSIONS

Monte Carlo simulation coupled with SEM is applied to study the variation in the high frequency response of a metallic beam and rod with the variation in the material properties. It can be seen that the method, which uses SEM is efficient and is taking only very less time than that of the time taken by the method using the conventional FEM. The ratio of the CPU time taken for a conventional FEM to the SEM increases with the loading frequency (here, it increases from 8 to 48 by increasing the frequency content of the load from 5 kHz to 50 kHz). The increase in the number of random variables used affects the responses considerably, only when the coefficient of variation is large. The change in

the variation of the time response and the dispersion relations, with the increase in the frequency, is purely depending on the uncertain input parameters considered . Regardless of the input parameter distributions considered, the maximum and minimum bound of the time for first reflection and the wavenumber variation distributions almost matches in all the cases. The variation of the shear mode in the beam and the contraction mode in the higher order rod suggests that the uncertainty enforces the use of higher order theories at low frequencies than the expected frequency, even for thin structures.

Finally, at this stage, it is very difficult to determine the reason for the shift in the arrival of the first reflection. For understanding the shift due to damage, uncertainties in damage location, its size and the type of damage also needs to be introduced in the formulation. This is indeed an open area of research and the author's are working towards the next research article focusing this very concept.

Acknowledgement

The authors would like to acknowledge the Boeing Aircraft Company, (Chicago, IL), for supporting this work. We are also thankful to Mr. Edward White from Boeing company, for his valuable suggestions to improve the quality of this work.

References

[Ang and Tang 1975] A.H.S. Ang, W.K. Tang, *Probability concepts in engineering planning and design, Volumes 1, Basic principles*, Wiley, New York, 1975.

[Antonella and Karam 2009] A.Antonella Cecchi, Karam Sab, "Discrete and continuous models for in plane loaded random elastic brickwork", *Eur. J. Mech. A/Solids* 28: 3 (2009), 610-625.

[Basudeb and Subrata 2002] B. Basudeb,C. Subrata, "NE MCS technique for stochastic structural response sensitivity", *Comput. Meth. Appl. Mech- Eng.* 191: 49-50 (2002), 5631-5645.

[Chakraborty and Gopalakrishnan 2004] A. Chakraborty, S. Gopalakrishnan, "A higher order spectral element formulation of functionally graded materials", *Acta mech.* 172: 1-2 (2004), 17-43.

[Decker 1991] M. K. Decker, "The Monte-carlo theory in science and engineering:Theory and application", *Comp. methods in Appl. Mech. Eng.* 89:1 (1991), 463-483.

[Doyle 1997] J.F Doyle, *Wave Propagation in Structures: Spectral Analysis Using Fast Discrete Fourier Transforms*, Springer-Verlag, New York, 1997.

[Ghanem and Spanos 2003] R.G. Ghanem, P.D. Spanos, *Stochastic finite elements: A Spectral Approach*, Dover, Newyork, 2003.

[Gopalakrishnan et al. 2008] S. Gopalakrishnan, A. Chakraborty, D.R. Mahapatra, *Spectral Finite Element Method*, Springer-Verlag, New York, 2008.

[Horr and Safi 2003] A.M. Horr, M.Safi, "Full dynamic analysis of offshore platform structures using exact Timoshenko pipe element", *Transactions of the ASME* 125:3 (2003), 168-175.

[James 1980] F. James, "Monte Carlo theory and practice", *Rep.Prog.Physics* 43:9 (1980), 1146-1188.

[Klieber and Hein 1992] R.G. Klieber, P.D. Hien, *The Stochastic finite element method; Basic Perturbation technique and Computer implementation*, Wiley publishers, England, 1992.

[Li and Chen 2006] J. Li, J.B. Chen, "The probability density evolution method for dynamic response analysis of non-linear stochastic structures", *Int. J. Numer. meth. eng.* 65:6 (2006), 882-903.

[Lepage 2006] S. Lepage, *Stochastic finite element method for the modeling of thermo elastic damping in micro-resonators*, Ph.D thesis,Universit de Lige, December, 2006.

[Liu et al. 1986a] W.K. Liu, Belytschko, A. Mani, "Probabilistic finite elements for non linear structural dynamics", *Comput. Methods Appl. Mech. Eng.* 56:1 (1986), 61-81.

[Liu et al. 1986b] W.K. Liu, Ted Belytschko, A. Mani, "Random finite elements", *Int. J. Numer. Meth. Eng.* 23:10 (1986), 1831-1845.

[Martin et al. [1994] M.A. Martin, S. Gopalakrishnan, J.F. Doyle, "Wave propagation in multiply connected deep waveguides" *J. Sound and Vibration* 174:4 (1994), 521-538.

[Mindlin and Herrmann 1950] R.D. Mindlin,G. Herrmann, "A one dimensional theory of compressional waves in an elastic rod", *Proceedings of First U.S. National Congress of Appl. mech.* (1950), 187-191.

[Nag et al. 2003] A. Nag, D.R. Mahapatra, S. Gopalakrishnan, T.S. Shankar, "A Spectral Finite Element with Embedded Delamination for Modeling Wave Scattering in Composite Beams", *Compos. Sci. Tech* 63:15 (2003), 2187-2200.

[Ostachowicz 2005] W. Ostachowicz, *Mechanics of the 21st Century*, Springer, Printed in the Netherlands, 2005, 275-286.

[Schueller 2001] G.I. Schueller, "Computational stochastic mechanics-recent advances", *Computers and Structures* 79:22 (2001), 2225-2234.

[Spanos and Zeldin 1998] P.D. Spanos, B.A. Zeldin, "Monte Carlo treatment of random fields: a broad perspective", *App. mech. rev.(ASME)* 51(1998), 219-237.

[Shinozuka 1972] M. Shinozuka, , "Monte-carlo solution of structural dynamics" *Computers and Structures* 2:5 (1972), 855-874 .

[Stefanou 2002] G. Stefanou, "The Stochastic Finite Element Method:Past present and future", *Comput. Meth. Appl. Mech. Eng.* 198:9 (2009), 1031-1051.

[Tracy and Padoen 1989] J.J. Tracy, G.C. Padoen, "Effect of Delamination on the natural frequencies of the composite laminates", *J. Compos. Mater.* 23:12 (1989), 1200-1215.

[Vinckenroy 1995] G. V. Vinckenroy, W.P. De Wilde, "The use of Monte Carlo techniques in statistical finite element methods for the determination of the structural behaviour of composite materials structural components.", *Composite structures* 32:1 (1995), 247-253.

Department of Aerospace engineering, Indian Institute of Science., Bangalore-560012, India

E-mail address: V. Ajith: ajith@aero.iisc.ernet.in

Department of Aerospace engineering, Indian Institute of Science., Bangalore, 560012, India

E-mail address: S. Gopalakrishnan: krishnan@aero.iisc.ernet.in